

Structure, Bonding, and Relative Stability of the Ground and Low-Lying Electronic States of CuO₂. The Role of Exact Exchange

Mireia Güell,[†] Josep M. Luis,[†] Luí Rodríguez-Santiago,[‡] Mariona Sodupe,[‡] and Miquel Solà^{*†}

Institut de Química Computacional and Departament de Química, Universitat de Girona, Campus de Montilivi E-17071, Girona, Catalonia, Spain, and Departament de Química, Universitat Autònoma de Barcelona, Bellaterra, E-08193 Barcelona, Spain

Received: April 11, 2008; Revised Manuscript Received: November 27, 2008

The C_{2v} and C_s ground and low-lying states of doublet CuO₂ are examined for a series of different density functionals (pure, hybrid, and meta-hybrid) and CCSD(T) methods. The effect of changing the B3LYP functional a₀ parameter is also explored. CCSD(T) results at the complete basis set limit show that the relative stability of the different electronic states is ²A₂(C_{2v}) < ²A''(C_s) < ²B₂(C_{2v}) < ²A'(C_s) ≪ ²A₁(C_{2v}) < ²B₁(C_{2v}). Unlike CCSD(T), all DFT methods analyzed in this work erroneously predict the end-on ²A'' state as the ground state for CuO₂ irrespective of the type of functional and percentage of Hartree–Fock (exact) exchange included in the B3LYP-like functional. Among the different functionals tested, B3LYP gives the best geometries and relative energies for the different electronic states when compared to CCSD(T) results. As for the effect of the a₀ parameter, it is found that the B3LYP-like functional yielding better geometries contains 20% of exact exchange, although somewhat unexpectedly, the B3LYP-like functional with a larger contribution of exact exchange (90%) is the one that gives the smaller standard deviation for relative energies.

INTRODUCTION

Copper, despite its toxicity in pure form, is fundamental for the activity of many enzymes, which are important in oxygen transport and insertion, electron transfer, redox processes, and so forth.^{1–5} One of the most important enzymes in humans that contains copper in the active site is the superoxide dismutase (SOD).⁶ This enzyme provides cellular defense against the oxidative stress by catalyzing O₂^{•-} disproportionation into the less toxic dioxygen and hydrogen peroxide:



The copper site is at the heart of the enzymatic active site of the SOD protein. The catalysis is a two-step process: one molecule of superoxide first reduces Cu²⁺ to form dioxygen and then a second molecule of O₂^{•-} reoxidizes Cu⁺ to form hydrogen peroxide (see Figure 1).^{7,8}

In order to study theoretically the mechanism for the toxic superoxide radical disproportionation by SOD, it is necessary to employ methods that describe correctly the interaction between copper ions (Cu⁺ and Cu²⁺) and the superoxide radical (O₂^{•-}). Most of the articles that study catalytic mechanisms computationally in enzymes use density functional theory (DFT) methods.^{9–12} DFT is the usual method of choice for studies of enzymatic or organometallic catalytic reaction mechanisms because the current hybrids or meta-GGA functionals provide, in general, similar or even better results on geometries and relative energies compared to correlated *ab initio* calculations such as MP2 while using less computer time.^{9–12} Unfortunately, however, this is not always the case. For instance, recently, some of us showed that many DFT methods fail to predict the correct ground electronic state of Cu²⁺–H₂O.¹³ This is due to the fact that, in certain electronic states, there is an important charge

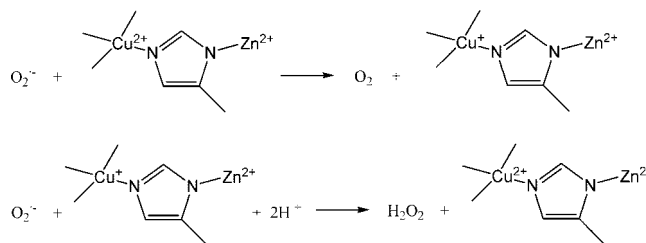


Figure 1. Mechanism for the disproportionation of superoxide to give dioxygen and hydrogen peroxide in superoxide dismutase.

and spin delocalization. These situations, as for two-center–three-electron (2c–3e) bond systems,^{14–16} have been shown to be overstabilized by most pure density functionals. For this reason, it was also found that the relative stability of the different electronic states in Cu²⁺–H₂O strongly depends on the degree of mixing of exact HF and DFT exchange functionals.¹³ Among the different functionals tested in that work,¹³ the BHandHLYP functional was found to be the one that provides better results compared to CCSD(T).

Before starting the investigation of any reaction mechanism involving Cu⁺– or Cu²⁺–O₂^{•-} species with DFT methods, it is convenient to make a detailed study of the performance of different DFT methods for the description of the geometry and energetics of the ground and low-lying states of CuO₂ and CuO₂⁺. This is the main goal pursued by the present paper. Hartree–Fock (HF) and coupled cluster with single and double excitations¹⁷ with the perturbation theory to include the effect of triple excitations¹⁸ (CCSD(T)) calculations with a complete basis set (CBS) extrapolation will be also carried out to get reference values to which our DFT results can be compared. Preliminary calculations of the singlet and triplet CuO₂⁺ species show that, qualitatively, the DFT relative energies of the ground and low-lying electronic states follow the same trends as those provided by the CCSD(T) method. For this reason, the present

* Corresponding author. E-mail: miquel.sola@udg.edu.

[†] Universitat de Girona.

[‡] Universitat Autònoma de Barcelona.

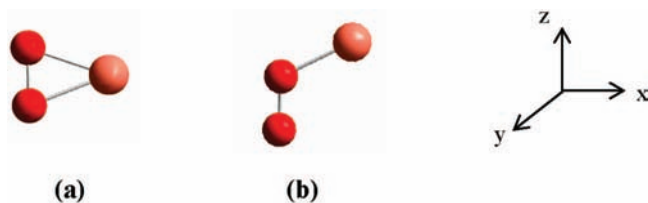


Figure 2. (a) Side-on (C_{2v}) and (b) end-on (C_s) structures of CuO₂.

paper is focused on the capability of DFT to provide the right energetic order and geometry (end-on C_s or side-on C_{2v} , Figure 2) of the ground and low-lying states of the doublet CuO₂. Quartet states of CuO₂ have not been considered here because they are basically van der Waals complexes far less stable than doublet states.^{19,20} For doublet CuO₂ species, we will also analyze the effect of changing the amount of HF exchange included in the B3LYP functional. Let us mention here that several benchmarks on the performance of different functionals for the study of inorganometallic and organometallic complexes are available in the literature.^{21–27}

The CuO₂ species has been extensively studied both experimentally and theoretically. It is known that a Cu(O₂) (hereafter referred as CuO₂) weakly bound complex is formed when Cu reacts with O₂ in rare-gas matrices.^{20,28–33} The linear OCuO dioxide that is formed after irradiation in the ultraviolet³⁴ is more strongly bound but it is less stable and will not be studied in the present work. Interestingly, the global minima on the M + O₂ potential energy surfaces (PESs) of all first-row transition metals correspond to the dioxide structure, the only exception being the CuO₂ with a superoxide structure.³⁵ Mitchell has determined that the bond dissociation in the ground-state angular CuO₂ is 15 ± 5 kcal mol⁻¹.³⁶ On the other hand, EPR experiments^{29–31} indicate two magnetically inequivalent oxygen atoms, and this has been interpreted in terms of an end-on C_s coordination (see Figure 2) for the ground state of CuO₂. HF³⁷ and DFT(B3LYP)^{19,20,38} studies reinforce this result by showing that the end-on C_s structure is about 10 kcal mol⁻¹ more stable than the side-on C_{2v} species. However, at the ab initio correlated level (MRCI,³⁹ CASPT2,³⁷ and CCSD(T)^{40,41} calculations) the side-on structure is found to be the ground state, with the end-on isomer being almost isoenergetic (only about 1 kcal mol⁻¹ less stable). One of us⁴⁰ attributed the difference between EPR results and theoretical predictions by high-level calculations to matrix effects taking place in EPR experiments that could either change the relative stabilities or produce an external magnetic field that causes the oxygen atoms of the C_{2v} side-on structure to be magnetically inequivalent. More recent calculations by Roos et al.³⁷ provided further support for the larger stabilization of the C_s as compared to the C_{2v} structure in rare-gas matrices, due to its larger dipole moment.

As said before, in the present work we address the effect of varying the fraction of exact HF exchange included in hybrid B3LYP-like functional on the relative energy and geometry of the ground and low-lying states of doublet CuO₂. The effect of changing the amount of HF exchange included in the B3LYP functional in the molecular structure,^{42–47} vibrational frequencies,^{45,47} first-order density,⁴⁸ thermochemistry and energy barriers,^{42,49–53} ionization potentials,⁵⁴ hydrogen bond infrared signature,⁵⁵ and nuclear resonance shielding constants⁵⁶ of several species has been discussed in previous works.^{42–56} Furthermore, Reiher and co-workers⁵⁷ have analyzed the importance of the admixture of exact HF exchange in the functional on the relative energy between electronic states of different multiplicities. These authors have shown that high-spin states in Fe(II)–sulfur

complexes are stabilized when the degree of exact HF exchange is increased and that the energy splitting between low-spin and high-spin states depends *linearly* on the coefficient of the HF exchange admixture. Because of problems with the B3LYP functional⁵⁸ for providing the spin ground state of iron–sulfur complexes, Reiher and co-workers⁵⁷ therefore proposed to lower the amount of HF exchange in B3LYP to 15%. This reparametrized functional, called B3LYP*, was indeed shown to afford better relative energies between electronic states as compared to B3LYP, but still failed for spin-crossover systems.⁵⁹ More recently, validation studies of DFT functionals⁶⁰ have shown the excellent performance of the OPBE and OLYP^{61–63} functionals for these spin-state splittings. These functionals will be included in our study.

Up to date, the CuO₂ molecule has been studied by DFT methods with only the B3LYP^{20,38} and the PW GGA-II functionals.¹⁹ In the present work, we will consider a wider series of functionals of different types (pure, hybrid, and meta-hybrid) as well as a set of B3LYP-like functionals with different degrees of HF exchange incorporation.

METHODOLOGY

HF, CCSD(T), and DFT calculations on geometries, energies, and harmonic vibrational frequencies of the C_s $^2A''$ and $^2A''$ and C_{2v} 2A_2 , 2B_2 , 2A_1 , and 2B_1 electronic states of the doublet CuO₂ species have been performed within the unrestricted formalism using the Gaussian 03 package program⁶⁴ for the HF and DFT methods and with the Molpro 2006.1 for the CCSD(T) calculations.⁶⁵ The S^2 expectation value (for DFT, this value is obtained using a Slater determinant constructed with the Kohn–Sham orbitals as approximate wave function) is, with few exceptions, close to the expected 0.75 value (see Table S1). CCSD(T) calculations have been done correlating all the electrons except the 1s electrons of O and the 1s, 2s, and 2p electrons of Cu. The 6-311+G(d) basis set as implemented in the Gaussian 03 has been used for all calculations. For Cu, this basis corresponds to the (14s9p5d)/[9s5p3d] Wachters basis set⁶⁶ with the contraction scheme 611111111/51111/311 supplemented with one s, two p, and one d diffuse functions and one f polarization function.⁶⁷ Moreover, single-point CCSD(T) energy calculations at the optimized CCSD(T)/6-311+G(d) geometry were carried out with the Dunning's aug-cc-pVTZ and aug-cc-pVQZ basis sets.⁶⁸ From these results we provide an estimation using eq 7 of ref 69 of the CCSD(T) energy extrapolated to a CBS limit. This equation has been employed to extrapolate both the HF and the correlation energy. For the two lowest energy states, we have performed additional geometry optimizations with the Dunning's aug-cc-pVTZ and aug-cc-pVQZ basis sets.⁶⁸

For the DFT calculations, we have used the Lee, Yang, and Parr (LYP)⁷⁰ correlation functional combined with the nonlocal hybrid Becke's three-parameter exchange functional (B3).⁵⁸ The B3 method was originally formulated as:⁵⁸

$$E_{XC} = E_X^{\text{LSDA}} + a_0(E_X^{\text{exact}} - E_X^{\text{LSDA}}) + a_x \Delta E_X^{\text{B88}} + a_c \Delta E_c^{\text{PW91}} \quad (2)$$

The E_X^{exact} , E_X^{LSDA} , ΔE_X^{B88} , and ΔE_c^{PW91} terms are the HF exchange energy based on Kohn–Sham orbitals, the uniform electron gas exchange–correlation energy, Becke's 1988 gradient correction for exchange,⁷¹ and the 1991 Perdew and Wang gradient correction to correlation,^{72–75} respectively. Commonly, this procedure is referred to as the B3PW91 method. The coefficients a_0 , a_x , and a_c were determined by Becke⁵⁸ by a linear

TABLE 1: Optimized Geometric Parameters^a of the Ground and Low-Lying Electronic States of CuO₂ at Different Levels of Theory Obtained with the 6-311+G(d) Basis Set

symmetry	state	geometry	HF	BLYP	G96LYP	OLYP	OPBE	mPWPW91	B3LYP	B3LYP*	BHandH	M05	VSXC	HCTH	TPSS	CCSD(T)
C_s	$^2A''$	R_{Cu-O}^b	1.915	1.907	1.906	1.974	1.940	1.893	1.911	1.904	1.839	1.907	1.922	1.946	1.876	1.878
		R_{O-O}	1.299	1.303	1.299	1.276	1.262	1.288	1.283	1.285	1.271	1.271	1.285	1.262	1.298	1.330
		α_{CuOO}	110.0	119.6	119.6	120.2	120.3	119.6	117.9	118.4	114.2	117.1	117.2	120.4	118.6	108.9
	$^2A'$	R_{Cu-O}^b	1.900	1.825	1.820	1.838	1.824	1.810	1.826	1.821	1.798	1.839	2.051	2.105	1.967	1.849
		R_{O-O}	1.313	1.358	1.353	1.328	1.312	1.341	1.341	1.342	1.301	1.312	1.247	1.228	1.260	1.370
		α_{CuOO}	113.4	115.5	115.6	118.1	118.3	115.6	114.0	114.4	114.2	116.0	118.4	124.4	125.2	100.3
C_{2v}	2A_2	R_{Cu-O}	2.070	2.007	2.000	2.018	2.003	1.990	2.009	2.004	1.968	2.024	2.011	2.014	1.983	2.014
		R_{O-O}	1.294	1.412	1.406	1.377	1.359	1.392	1.364	1.371	1.307	1.331	1.386	1.362	1.397	1.374
		α_{CuOO}	71.8	69.4	69.4	70.0	70.2	69.5	70.2	70.0	70.6	70.8	69.8	70.2	69.4	70.1
	2B_2	R_{Cu-O}	2.091	1.925	1.918	1.934	1.915	1.907	1.952	1.937	1.841	1.974	1.935	1.934	1.900	1.981
		R_{O-O}	1.308	1.469	1.462	1.425	1.404	1.447	1.401	1.413	1.330	1.358	1.435	1.408	1.455	1.398
		α_{CuOO}	71.8	67.6	67.6	68.4	68.5	67.7	69.0	68.6	70.0	69.9	68.2	68.7	67.5	69.3
	2A_1	R_{Cu-O}	2.036	2.039	2.026	2.063	2.010	1.998	2.022	2.016	1.938	2.220	2.047	2.117	1.967	1.931
		R_{O-O}	1.304	1.316	1.313	1.285	1.277	1.305	1.275	1.284	1.225	1.230	1.288	1.263	1.314	1.315
		α_{CuOO}	71.3	71.2	71.1	71.8	71.5	70.9	71.6	71.4	71.6	73.9	71.7	72.7	70.5	70.1
	2B_1	R_{Cu-O}	1.830	— ^c	— ^c	1.893	1.878	— ^c	1.875	1.877	1.795	1.879	1.888	1.892	1.860	1.912
		R_{O-O}	1.522	— ^c	— ^c	1.777	1.735	— ^c	1.711	1.727	1.566	1.653	1.812	1.770	1.805	1.939
		α_{CuOO}	65.4	— ^c	— ^c	62.0	62.5	— ^c	62.9	62.6	64.1	63.9	61.3	62.1	61.0	61.0

^a Distances are in angstroms and angles in degrees. ^b Cu–O bond length corresponding to the shortest Cu–O distance. ^c The SCF process in this state could not be converged.

least-squares fit to 56 experimental atomization energies, 42 ionization potentials, and 8 proton affinities. The values thus obtained were $a_0 = 0.20$, $a_x = 0.72$, and $a_c = 0.81$. In the Gaussian 03⁶⁴ implementation, the expression of the B3LYP functional is similar to eq 2 with some minor differences:⁷⁶

$$E_{XC} = E_X^{LSDA} + a_0(E_X^{\text{exact}} - E_X^{LSDA}) + a_x \Delta E_X^{\text{B88}} + E_C^{\text{VWN}} + a_c(\Delta E_C^{\text{LYP}} - E_C^{\text{VWN}})(3)$$

In this equation, the Perdew and Wang correlation functional originally used by Becke is replaced by the Lee–Yang–Parr (LYP)⁷⁰ one. Since the LYP functional already contains a local part and a gradient correction, one has to remove the local part to obtain a correct implementation. This can be done in an approximate way by subtracting E_C^{VWN} from ΔE_C^{LYP} . Note that in the Gaussian 03 implementation the VWN functional is the one derived by Vosko et al. from a fit to the random phase approximation^{77,78} results. It is also worth noting that the set of parameters $a_0 = 1.0$, $a_x = a_c = 0$ does not reproduce the HF results due to the presence of the E_C^{VWN} term in eq 3.

Besides these functionals, others have also been tested. First, we have used the pure exchange functional OPTX⁶¹ combined with the LYP⁷⁰ (OLYP) and PBE^{62,79} (OPBE) correlation functionals as well as the pure BLYP,⁷¹ G96LYP,⁸⁰ and mPWPW91.⁸¹ Second, we have employed the hybrids B3LYP*,⁵⁷ which uses 15% Hartree–Fock exchange compared to the 20% used in the original B3LYP, and Becke’s half-and-half method (BHandH),⁸² which also makes use of eq 3 with $a_0 = 0.5$, $a_x = 0.5$, and $a_c = 0$. Finally, we have tested four meta-hybrid functionals, the M05,⁸³ VSXC⁸⁴ HCTH/407,⁸⁵ and TPSS⁸⁶ functionals. According to Zhao, Schultz, and Truhlar,⁸⁷ the BLYP, G96LYP, PBE, mPWPW91, and M05 are the most efficient functionals for the description of transition metal–ligand and transition metal–transition metal bond energies.

RESULTS AND DISCUSSION

Cu^+ is one of the two most common ions formed by copper. Its electron configuration is $4s^0 3d^{10}$, and it is a diamagnetic ion. The superoxide anion is the product of the one-electron reduction of dioxygen, which occurs widely in nature. With one unpaired electron, the superoxide ion is a free radical, and, like dioxygen, it is paramagnetic. When Cu^+ and the superoxide anion are combined, the doublet CuO_2 molecule is obtained. We have

performed geometric optimizations and frequency calculations for doublet CuO_2 in different C_s and C_{2v} electronic states (Figure 2). It is worth mentioning here that previous MRSDCI calculations³⁹ proved that in the C_s $^2A''$ and $^2A'$ states (and therefore most likely in the C_{2v} 2A_2 and 2B_2 states, *vide infra*) the RHF configuration dominates the final wave function. Therefore, it is expected that the single reference based CCSD(T) method yields an accurate description of these electronic states. Indeed, the test T1⁸⁸ that provides an estimation of the importance of static correlation is never larger than 0.06 for all analyzed electronic states, except for the highest 2B_1 one, for which T1 is 0.11. Consequently, nondynamical correlation may be important for this state. Note that in the 2B_1 electronic state metal inserts into the O_2 bond (*vide infra*).

A. CuO_2 Description by the HF, CCSD(T), and Standard DFT Methods. Table 1 contains the optimized geometrical parameters of the ground and low-lying electronic states of CuO_2 doublet obtained with HF, BLYP, G96LYP, OLYP, OPBE, mPWPW91, B3LYP, B3LYP*, BHandH, M05, VSXC, HCTH, and TPSS and the highly correlated CCSD(T) post-HF-method using the 6-311+G(d) basis set for the C_s and C_{2v} low-lying electronic states. In Table 2, the standard deviations for the optimized geometries obtained with the different methods as compared to the CCSD(T)/6-311+G(d) results are given. Table 3 shows the relative energies obtained with these different methods, while Table 4 contains the same relative energies computed with the CCSD(T) method theory using the aug-cc-pVTZ and aug-cc-pVQZ basis sets as well as an estimation of the CCSD(T) energy extrapolated to the CBS limit at the CCSD(T)/6-311+G(d) optimized geometries. Finally, Table 5 lists the geometrical parameters and relative energies of the two lowest-energy states computed at the CCSD(T) level with the aug-cc-pVTZ and aug-cc-pVQZ basis sets together with an estimation of the CCSD(T) relative energy extrapolated to the CBS limit obtained using the CCSD(T)/aug-cc-pVQZ geometry.

The calculated B3LYP molecular orbitals (MOs) for the different electronic states and the qualitative MO diagram for the interaction between the Cu (2S) and O_2 ($^3\Sigma_g^-$) fragments in the side-on C_{2v} CuO_2 species are given in Tables S3–S8 and Figure S1, respectively, of the Supporting Information. Bonding orbitals for side-on CuO_2 are located well below the HOMO, while the upper levels, which are either nonbonding or antibonding, exhibit small Cu– O_2 overlaps.¹⁹ For the C_{2v} species,

TABLE 2: Standard Deviation Values (STD) for the Geometric Parameters^a of CuO₂ in Different Electronic States with the 6-311+G(d) Basis Set

symmetry	state	HF	BLYP	G96LYP	OLYP	OPBE	mPWPW91	B3LYP	B3LYP*	BHandH	M05	VSX	HCTH	TPSS
C_s	$^2A''$	0.030	0.110	0.111	0.131	0.127	0.111	0.097	0.101	0.067	0.091	0.092	0.129	0.100
	$^2A'$	0.139	0.154	0.155	0.181	0.185	0.157	0.140	0.144	0.149	0.162	0.228	0.296	0.268
C_{2v}	2A_2	0.059	0.023	0.021	0.003	0.011	0.018	0.007	0.006	0.047	0.027	0.008	0.007	0.023
	2B_2	0.086	0.055	0.054	0.033	0.039	0.054	0.017	0.028	0.090	0.024	0.036	0.028	0.060
	2A_1	0.062	0.063	0.056	0.080	0.053	0.040	0.059	0.054	0.054	0.178	0.071	0.115	0.021
	2B_1	0.250	— ^b	— ^b	0.095	0.120	— ^b	0.135	0.125	0.228	0.169	0.075	0.099	0.083
mean		0.104	0.081	0.080	0.087	0.089	0.076	0.076	0.076	0.106	0.108	0.085	0.112	0.093
mean— 2B_1 ^c		0.075	0.081	0.080	0.086	0.083	0.076	0.064	0.067	0.082	0.096	0.087	0.115	0.094

^a For the calculation of the STD we have used the distances in angstroms and angles in radians. STD values have been calculated as $(\sum_{i=1}^N (d_i^{\text{Level of theory}} - d_i^{\text{CCSD(T)}})^2/N)^{1/2}$ with $N = 3$ ($R_{\text{Cu-O}}$, $R_{\text{O-O}}$, α_{CuOO}). ^b The SCF process in this state could not be converged. ^c The results of the 2B_1 state are not taken into account in the calculation of the STD.

TABLE 3: Relative Energies (in kcal mol⁻¹) of the Ground and Low-Lying Electronic States of CuO₂ at Different Levels of Theory with the 6-311+G(d) Basis Set

symmetry	state	HF	BLYP	G96LYP	OLYP	OPBE	mPWPW91	B3LYP	B3LYP*	BHandH	M05	VSX	HCTH	TPSS	CCSD(T)
C_s	$^2A''$	0.00	0.00	0.00	0.00	0.00	0.00	0.00	0.00	0.00	0.00	0.00	0.00	0.00	0.03
	$^2A'$	3.77	17.50	17.44	18.26	18.31	17.46	13.41	14.53	8.63	13.05	47.77	18.99	42.85	8.49
C_{2v}	2A_2	1.72	14.83	14.63	15.27	14.49	13.97	8.98	10.27	2.02	8.30	8.01	15.84	10.88	0.00
	2B_2	7.31	19.76	19.48	21.30	20.35	18.79	15.37	16.37	9.46	15.90	15.03	22.57	14.62	7.86
	2A_1	20.57	46.35	46.21	49.39	48.26	45.14	50.30	48.92	56.86	57.55	49.62	53.33	43.40	40.66
	2B_1	81.16	— ^b	— ^b	73.49	75.90	— ^b	77.18	74.71	89.46	85.11	66.35	76.54	64.63	66.93
STD ^a		10.26	9.75	9.59	10.23	10.01	9.11	7.74	7.56	11.38	11.33	17.03	11.76	15.04	—
mean— 2B_1 ^c		9.26	9.75	9.59	10.82	10.20	9.11	7.13	7.52	7.34	9.38	18.65	12.15	16.44	—

^a Standard deviation values have been calculated as $(\sum_{i=1}^N (E_i^{\text{Level of theory}} - E_i^{\text{CCSD(T)}})^2/N)^{1/2}$ with $N = 6$ ($E(^2A'')$, $E(^2A')$, $E(^2A_2)$, $E(^2B_2)$, $E(^2A_1)$, $E(^2B_1)$). ^b The SCF process in this state could not be converged. ^c The results of the 2B_1 state are not taken into account in the calculation of the STD.

TABLE 4: Relative Energies (in kcal mol⁻¹) of the Ground and Low-Lying Electronic States of CuO₂ at CCSD(T) Level of Theory with Different Basis Sets at the Optimized CCSD(T)/6-311+G(d) Geometry

symmetry	state	aug-cc-pVTZ	aug-cc-pVQZ	CBS limit
C_s	$^2A''$	1.38	1.38	1.38
	$^2A'$	9.34	9.33	9.33
C_{2v}	2A_2	0.00	0.00	0.00
	2B_2	6.96	6.95	6.94
	2A_1	40.02	40.48	40.82
	2B_1	71.08	73.19	74.73

TABLE 5: Optimized Geometric Parameters of the Two Lowest Electronic States (2A_2 and $^2A''$) and Relative Energy (ΔE , kcal/mol) of the $^2A''$ with Respect to the 2A_2 Electronic States of CuO₂ at the CCSD(T) Level of Theory with the aug-cc-pVTZ and aug-cc-pVQZ Basis Sets

	state	geometry	aug-cc-pVTZ	aug-cc-pVQZ
C_{2v}	2A_2	$R_{\text{Cu-O}}$	1.986	1.982
		$R_{\text{O-O}}$	1.377	1.370
		α_{CuOO}	69.7	69.8
C_s	$^2A''$	$R_{\text{Cu-O}}$	1.857	1.854
		$R_{\text{O-O}}$	1.341	1.336
		α_{CuOO}	104.1	103.2
ΔE			1.39	1.38
ΔE (CBS limit)			—	1.38

we have analyzed the lowest-lying 2A_2 , 2B_2 , 2A_1 , and 2B_1 electronic states. The results show that in the 2A_2 state the singly occupied MO (SOMO) is the $2a_2$ orbital, which is an antibonding combination of the copper d_{yz} orbital with the π^* out-of-plane antibonding MO of O₂, the latter having a larger amplitude. The SOMO in the 2B_2 state is the $6b_2$ orbital formed the antibonding combination of a small portion of the copper d_{xz} orbital and a large contribution of the in-plane O₂ π^* antibonding MO. In the 2A_1 state, the SOMO ($12a_1$) corresponds basically to a combination of the $4s$ and $4p_x$ copper MOs. Finally, in the

2B_1 state, the SOMO ($4b_1$) is an antibonding combination of the copper d_{xy} orbital with the out-of-plane O₂ π bonding MO.

The C_{2v} form of CuO₂ can be transformed into the C_s isomer by simply moving the O₂ moiety along the z -axis (see Figure 2). This movement connects the 2A_2 and 2B_2 states of the C_{2v} symmetry species with the $^2A''$ and $^2A'$ states in the C_s structure, respectively. In the $^2A''(C_s)$ state, the SOMO ($6a''$) mainly corresponds to the antibonding combination of the d_{yz} and $d_{x^2-y^2}$ orbitals for the copper with the π^* out-of-plane antibonding MO of O₂, the latter with a larger coefficient. In the $^2A'(C_s)$ state, the SOMO ($17a'$) is formed by the combination of the d_{xy} and d_{yz} orbitals of the copper with a small coefficient and a large contribution of the in-plane O₂ π^* antibonding MO. These $6a''$ and $17a'$ MOs are closely related to the C_{2v} $2a_2$ and $6b_2$ MOs, respectively. As we will see next, the energy differences between $^2A''$ and 2A_2 and also between $^2A'$ and 2B_2 are in general small for all methods of calculation analyzed. Indeed, an exceedingly flat PES is found in the direction that transforms the 2A_2 C_{2v} stationary point into the $^2A''$ C_s minimum.^{37,40,41}

In all states (except for the 2A_1), the Cu—O₂ interaction is characterized by the drop of the unpaired $4s$ electron of Cu to the π^* antibonding MOs of O₂.^{38,40} So, the bonding is essentially ionic ($\text{Cu}^+ - \text{O}_2^-$) with some covalent contributions coming basically from the interactions between the O₂ π^* MOs and the Cu unoccupied $4p$ orbitals of suitable symmetry.⁴⁰ Interestingly, in the C_s structure the $4s$ Cu orbital can participate in the mixing, and, therefore, the end-on structure has a somewhat large covalent character^{38,40} as can be corroborated by the Mulliken charges on Cu atoms given in Table S8 of the Supporting Information.

With respect to the geometrical parameters, Table 1 shows that the changes of the α_{CuOO} angle are especially important in the $^2A''$ electronic state ranging from 108.9° at the CCSD(T) level to 120.4° with the HCTC functional, as a consequence of the PES being very flat around the $^2A''$ minimum. The CCSD(T) optimized $R_{\text{O-O}}$ bond distance for $^2A''$ and 2A_2 is 1.330 and

1.374 Å, respectively. The larger value in the 2A_2 electronic state is a consequence of its higher ionicity which translates into larger $O_2 \pi^*$ population. These O–O bond lengths in CuO_2 are much closer to that of ${}^2\Pi_g O_2^-$ (exptl, 1.35 Å;⁸⁹ CCSD(T), 1.354 Å) than that of neutral ${}^3\Sigma_g^- O_2$ (exptl, 1.208 Å;⁸⁹ CCSD(T), 1.211 Å) for most of the electronic states analyzed and theoretical methods used (see Table S10 in the Supporting Information) as expected from the essential ionic nature of the chemical bond in CuO_2 . This is also reflected in the harmonic frequencies corresponding to the O–O stretching (see Tables S11–S17 of the Supporting Information). For the 2A_1 state, the O–O bond length is the shortest at the CCSD(T) level, which is not unexpected given the fact that the SOMO in this state ($12a_1$) does not have O–O π^* antibonding contribution. Conversely, for the 2B_1 state, the O–O bond length is the longest at all levels of theory ranging from 1.939 Å in CCSD(T) to 1.522 Å in HF. The change from the 2A_2 to the 2B_1 electronic states involves the promotion of an electron from the $4b_1$ orbital, with an O–O π bonding contribution, to the $2a_2$ with an O–O π^* antibonding character. Consequently, there is an important increase in the R_{O-O} bond distance together with a reduction of the $\nu(O-O)$ harmonic frequency. In fact, in the 2B_1 stationary point, the O–O bond is broken and the CuO_2 complex has to be considered as an $OCuO$ angular species. For all cases, except for the 2A_2 state at the HF level and the ${}^2A''$ state computed with the VSXC, HCTH, and TPSS functionals, the R_{Cu-O} distance is slightly larger for the related ${}^2A''$ and 2A_2 than for the ${}^2A'$ and 2B_2 states, respectively. As discussed by Bauschlicher et al.,⁴⁰ this has to be ascribed to the lower Cu– O_2 Pauli repulsion in the ${}^2A'$ and 2B_2 states as a result of having three electrons (as opposed to four in the ${}^2A''$ and 2A_2 states) occupying in-plane $O_2 \pi^*$ orbitals. In spite of that, electrostatic interactions are more favorable when there are four electrons in the in-plane $O_2 \pi^*$ orbitals which explains the higher stability of the ${}^2A''$ and 2A_2 states as compared to the ${}^2A'$ and 2B_2 states, respectively (*vide infra*). Let us notice that for all states except the 2B_1 , there is a reduction of the Cu–O bond length when going from HF to CCSD(T) result. This behavior is opposed to the usual increase in the bond lengths when correlation effects are included, and it is likely to be the result of important contributions of the excitations starting from the $6b_2$ and $2a_2$ orbitals, of similar energies and Cu–O antibonding character, to orbitals of higher energy with Cu–O nonbonding character.

In Table 2, we list the standard deviation (STD) of the geometrical parameters given in Table 1 as compared to the CCSD(T)/6-311+G(d) optimized parameters in each state. This number gives an idea of the performance of the different functionals for geometric parameters. It is worth noting the relatively good behavior of the HF method for geometries (with the exception of the 2B_1 state for which nondynamical correlation could be important), which is not totally surprisingly given the well-known good performance of the HF method for ionic species. In spite of that, the HF results are outperformed by all DFT functionals except for the BHandH, M05, and HCTH, which show a similar performance to that of the HF method.

It can be observed in Table 3 that, at the CCSD(T)/6-311+G(d) level, the ground electronic state of CuO_2 doublet is the ${}^2A_2(C_{2v})$ and the relative stability of the different electronic states is ${}^2A_2(C_{2v}) < {}^2A''(C_s) < {}^2B_2(C_{2v}) < {}^2A'(C_s) \ll {}^2A_1(C_{2v}) < {}^2B_1(C_{2v})$. The same relative stability order is obtained with single-point energies calculations at the optimized CCSD(T)/6-311+G(d) geometries using the aug-cc-pVTZ and aug-cc-pVQZ basis sets and extrapolating to the CBS limit. At the CBS limit (Table 4), the energy difference between 2A_2 and ${}^2A''$

increases from 0.03 to 1.4 kcal mol⁻¹. In Table 5 we provide the geometries and energy differences found with the CCSD(T) method using the aug-cc-pVTZ and aug-cc-pVQZ basis sets. As can be seen, in comparison with the 6-311+G(d) results, the Cu–O bond contracts by 0.02–0.03 Å with these basis sets, but energy differences remain unchanged. Our best estimate for the energy difference between the 2A_2 and the ${}^2A''$ lowest-energy states is 1.38 kcal mol⁻¹, the 2A_2 being the most stable. It is important to remark that this energy difference is converged with respect to the basis set (see Tables 4 and 5) and optimized geometry (compare the results with the CCSD(T)/6-311+G(d) and CCSD(T)/aug-cc-pVQZ geometries). The higher stability of the side-on 2A_2 as compared to end-on ${}^2A''$ species in the gas phase was already found previously at the CASPT2³⁷ and CCSD(T)^{40,41} correlated levels, the energy difference reported being similar to that found in the present study (CASPT2 = 0.5³⁷ kcal mol⁻¹; CCSD(T) = 0.74^{40,41} and 0.9^{40,41} kcal mol⁻¹). As said in the Introduction, EPR experiments^{29–31} show two magnetically inequivalent oxygen atoms, and this had been taken as an indication that the end-on C_s structure is the ground state. CASPT2 calculations by Roos et al.³⁷ indicate that the gas-phase ground state is the side-on 2A_2 state, but, because of the small energy difference between the two species, the ${}^2A'' C_s$ structure, which has a large dipole moment, becomes the ground state in rare-gas matrices.

The relative stability of the different electronic states found by the HF and DFT analyzed methods is ${}^2A''(C_s) < {}^2A_2(C_{2v}) < {}^2A'(C_s) < {}^2B_2(C_{2v}) \ll {}^2A_1(C_{2v}) < {}^2B_1(C_{2v})$. Unfortunately, for the BLYP, G96LYP, and mPWPW91 methods, we were unable to converge the 2B_1 state. As found in previous studies,^{19,20,37,38} our HF and DFT results indicate that the end-on C_s structure is more stable than the side-on C_{2v} species by about 10 kcal mol⁻¹. Only the HF and BHandH yield side-on ${}^2A_2(C_{2v})$ and end-on ${}^2A''(C_s)$ species of comparable energy (about 2 kcal mol⁻¹ difference). When all electronic states are considered, the standard deviation values (last row of Table 3) indicate that B3LYP and B3LYP* are the methods that globally give the more similar results to the data obtained using CCSD(T)/6-311+G(d). All STD given by the DFT methods are smaller than the HF STD except for the M05, VSXC, HCTH, and TPSS functionals. If we take the STD for all states except the 2B_1 , then only the mPWPW91, B3LYP, B3LYP*, and BHandH perform better than HF.

The side-on ${}^2A_2(C_{2v})$ and end-on ${}^2A''(C_s)$ species are almost isoenergetic according to our HF, BHandH, and CCSD(T) results. The fact that most DFT methods such as the B3LYP clearly favor by about 10 kcal mol⁻¹ the end-on ${}^2A''$ state as compared to 2A_2 one is due, in part, to the fact that the 2A_2 state has a larger ionic character (*vide supra*) than the ${}^2A''$ state. Therefore, its stability is underestimated by most DFT methods because these methods overestimate the Cu first IP (see Table S18; exptl, 7.72 eV;⁹⁰ CCSD(T)/CBS limit, 7.54 eV; CCSD(T)/6-311+G(d), 7.26 eV; B3LYP/6-311+G(d), 8.04 eV). Since the CCSD(T) method yields a low IP as compared to the experimental value, the possibility of the 2A_2 state being overstabilized by CCSD(T) methods cannot be ruled out.³⁸

Let us finish this section by analyzing the binding energies (BEs) of CuO_2 ground state with respect to the Cu (2S) and O_2 (${}^3\Sigma_g^-$) fragments for the different levels of calculation listed in Table 6. The considered CuO_2 ground state is ${}^2A''$ for HF and DFT methods and 2A_2 for the CCSD(T) method. This BE was measured experimentally by Mitchell to be 15 ± 5 kcal mol⁻¹.³⁶ The CCSD(T) result we have obtained with the aug-cc-pVTZ and aug-cc-pVQZ basis sets at their respective optimized

TABLE 6: Binding Dissociation Energies (kcal mol⁻¹) of CuO₂ in Its Electronic Ground State with the 6-311+G(d) Basis Set for Different Methods of Calculation Used

	G96-		mPWP-		BH-		CCSD-		CCSD-		CCSD-		exptl				
	HF	BLYP	LYP	OPBE	W91	B3LYP	B3LYP*	andH	M05	VSXC	HCTH	TPSS		(T) ^a	(T) ^b	(T) ^c	
BDE	-11.11	19.94	17.14	12.53	12.60	19.85	12.74	15.06	11.60	13.09	22.02	14.02	20.90	6.52	13.78	13.81	15 ± 5 ^d

^a 6-311+G(d) basis set. ^b aug-cc-pVTZ basis set. ^c aug-cc-pVQZ basis set. ^d From ref 36.

TABLE 7: Optimized Geometric Parameters^a of the Ground and Low-Lying Electronic States of CuO₂ Computed with the B3LYP Method Using Different Parameter Sets^b with Basis 6-311+G(d)

symmetry	state	geometry	parameter set										HF
			0	1	2	3	4	5	6	7	8	9	
<i>C_s</i>	² A''	<i>R</i> _{Cu-O} ^c	1.907	1.918	1.920	1.914	1.897	1.889	1.886	1.888	1.890	1.892	1.915
		<i>R</i> _{O-O}	1.303	1.293	1.286	1.285	1.291	1.294	1.293	1.290	1.285	1.280	1.299
		<i>α</i> _{CuOO}	119.6	118.7	117.8	116.8	115.1	113.4	112.0	110.7	109.8	109.5	110.0
	² A'	<i>R</i> _{Cu-O} ^c	1.825	2.013	1.834	1.840	1.846	1.852	1.859	1.865	1.870	1.875	1.900
		<i>R</i> _{O-O}	1.358	1.387	1.345	1.338	1.331	1.322	1.315	1.307	1.298	1.294	1.313
		<i>α</i> _{CuOO}	115.5	114.5	113.9	113.3	112.9	113.0	112.3	112.3	112.5	112.9	113.4
<i>C_{2v}</i>	² A ₂	<i>R</i> _{Cu-O}	2.007	2.013	2.018	2.022	2.025	2.029	2.032	2.035	2.039	2.041	2.070
		<i>R</i> _{O-O}	1.412	1.387	1.367	1.351	1.336	1.323	1.312	1.301	1.292	1.283	1.294
		<i>α</i> _{CuOO}	69.4	69.8	70.2	70.5	70.7	71.0	71.2	71.4	71.5	71.7	71.8
	² B ₂	<i>R</i> _{Cu-O}	1.925	1.942	1.963	1.984	2.000	2.014	2.027	2.035	2.042	2.049	2.091
		<i>R</i> _{O-O}	1.469	1.433	1.403	1.379	1.360	1.343	1.329	1.318	1.317	1.296	1.308
		<i>α</i> _{CuOO}	67.6	68.3	69.1	69.7	70.1	70.5	70.9	71.1	71.4	71.6	71.8
	² A ₁	<i>R</i> _{Cu-O}	2.039	2.037	2.053	2.035	1.997	1.979	1.990	1.986	1.995	1.995	2.036
		<i>R</i> _{O-O}	1.316	1.295	1.286	1.279	1.289	1.300	1.303	1.300	1.295	1.288	1.304
		<i>α</i> _{CuOO}	71.2	71.5	71.8	71.7	71.2	70.9	70.8	70.9	71.0	71.2	71.3
	² B ₁	<i>R</i> _{Cu-O}	— ^d	1.889	1.883	1.869	1.845	1.823	1.818	1.802	1.813	1.811	1.830
		<i>R</i> _{O-O}	— ^d	1.764	1.716	1.679	1.640	1.600	1.569	1.545	1.525	1.508	1.522
		<i>α</i> _{CuOO}	— ^d	62.2	62.9	63.3	63.6	64.0	64.4	64.8	65.1	65.4	65.4

^a Distances are in angstroms and angles in degrees. ^b Table S1. ^c Cu–O bond length corresponding to the shortest Cu–O distance. ^d This state cannot be converged with the BLYP functional (set 0).

geometries is 13.78 and 13.81 kcal mol⁻¹, in good agreement with the experimental value. Surprisingly, the BE obtained at the CCSD(T)/6-311+G(d) level is clearly too low by about 10 kcal mol⁻¹ in comparison to the experiment and the CCSD(T) result obtained at the CBS limit, which points out the importance of the basis set at this level of theory for obtaining an accurate binding energy. For the present system, and due to the nature of the bonding (Cu⁺–O₂⁻), it is particularly important to accurately describe the electron affinity (EA) of O₂, which at the CCSD(T) level requires large basis sets with multiple diffuse and polarization functions. Note that the CCSD(T) EA of O₂ is computed to be 0.03, 0.36, and 0.38 eV with the 6-311+G(d), aug-ccpVDZ, and aug-ccpVTZ basis sets, respectively, the experimental value being 0.448 ± 0.006 eV.⁹¹ Most functionals with the exception of VSXC give binding energies ranging from 10 to 20 kcal mol⁻¹ and therefore within the experimental result. On the contrary, the HF value of -11.1 kcal mol⁻¹ indicates that this method erroneously considers CuO₂ as a metastable species. As compared to the experimental value, the B3LYP* functional yields the closest result.

B. On the Optimal Mixing of HF Exchange in B3LYP-like Functionals for the CuO₂ Description. It is well-known that estimations of IPs are usually better when using hybrid methods with a large percentage (about 40%) of HF exchange.^{54,92} To explore whether hybrid methods with increasing degree of HF exchange can reproduce better the CCSD(T) results, we have calculated the different electronic states of CuO₂ doublet by varying monotonically the proportion of exact exchange introduced in B3LYP-like functionals. We have made use of the Gaussian 03 program feature that allows one to vary the B3LYP standard Becke parameter set (PS) through internal options.

We have changed the *a*₀ parameter by 0.100 increments in the interval 0.100 ≤ *a*₀ ≤ 0.900, with fixed *a*_x = 1 - *a*₀ and *a*_c

= *a*_x. The *a*_x = 1 - *a*₀ relationship has already been used in some hybrid functionals.^{79,93} We also found in previous works⁴⁸ that the *a*_x = 1 - *a*₀ and *a*_c = *a*_x relations between the B3LYP parameters are, on average, the optimal ones to minimize the difference between the actual B3LYP density and the QCISD one in a series of small molecules. For this reason the relationships between *a*_x and *a*₀ and *a*_c mentioned previously will be maintained throughout this work. However, neither the choice that we have employed here nor other possible alternative relations among the three parameters should be considered as universal.^{48,79} In Table S1, we list the different PSs {*a*₀, *a*_x, *a*_c} employed.

The optimized geometric parameters and the STD of the optimized geometrical parameters as a function of *a*₀ are collected in Tables 7 and 8, while Table 9 contains the relative energies of different electronic states obtained with the different PSs. The HF values have been included for comparison purposes. For the *C*_{2v} ²A₂ and ²B₂ states (and also for the related *C*_s ²A'' and ²A'), the *R*_{O-O} bond distance decreases with the increase of the *a*₀ parameter. In general, this is the expected behavior when increasing the portion of HF exchange⁴⁶ in the functional since HF distances are usually shorter than correlated ones. This reduction in the *R*_{O-O} bond distance goes with a steady increase in the *α*_{CuOO} angle when going from BLYP to HF. Finally, the Cu–O bond increases with the growth in the *a*₀ parameter, especially in the ²B₂ state. This is the result of the Cu–O bond distance being longer at the HF level, for the reasons discussed before. In addition, the Cu–O bond becomes more ionic when *a*₀ increases. The energy of the 4s Cu orbital keeps approximately constant while the O₂ π* orbitals are stabilized, so both orbitals become more distant in energy when *a*₀ increases, and this favors the charge transfer from Cu to O₂ for the *C*_{2v} ²A₂ and ²B₂ states. This is confirmed by the Mulliken

TABLE 8: Calculation of the STD of the Geometric Parameters of the Ground and Low-Lying Electronic States of CuO₂ Computed with the B3LYP Method Using Different Parameter Sets^a with Basis 6-311+G(d)

symmetry	state	parameter set										HF
		0	1	2	3	4	5	6	7	8	9	
C _s	² A''	0.110	0.104	0.097	0.086	0.068	0.050	0.039	0.030	0.028	0.031	0.030
	² A'	0.154	0.321	0.138	0.132	0.129	0.131	0.125	0.127	0.131	0.135	0.139
C _{2v}	² A ₂	0.023	0.008	0.005	0.015	0.024	0.032	0.039	0.046	0.052	0.057	0.059
	² B ₂	0.055	0.032	0.011	0.012	0.026	0.039	0.050	0.059	0.074	0.074	0.086
	² A ₁	0.063	0.064	0.075	0.066	0.042	0.030	0.035	0.034	0.040	0.042	0.062
	² B ₁	— ^{b,c}	0.103	0.131	0.154	0.179	0.205	0.223	0.239	0.249	0.259	0.250
mean		0.081	0.105	0.076	0.077	0.078	0.081	0.085	0.089	0.096	0.100	0.104
mean— ² B ₁ ^c		0.081	0.126	0.091	0.093	0.094	0.097	0.102	0.107	0.115	0.120	0.125

^a See Table S1. ^b This state cannot be converged with the BLYP functional (set 0). ^c The results of the ²B₁ state are not taken into account in the calculation of the STD.

TABLE 9: Relative Energies (in kcal mol⁻¹) of the Ground and Low-Lying Electronic States of CuO₂ Computed with the B3LYP Method Using Different Parameter Sets^a with Basis 6-311+G(d)

symmetry	state	parameter set										HF
		0	1	2	3	4	5	6	7	8	9	
C _s	² A''	0.00	0.00	0.00	0.00	0.00	0.00	0.00	0.00	0.00	0.00	0.00
	² A'	17.50	15.41	13.25	11.07	9.11	7.60	6.50	5.66	5.02	4.50	3.77
C _{2v}	² A ₂	14.83	11.80	9.04	6.52	4.43	2.95	1.98	1.36	0.98	0.78	1.72
	² B ₂	19.76	17.57	15.41	13.18	11.14	9.57	8.44	7.63	7.14	6.67	7.31
	² A ₁	46.35	48.09	50.33	51.89	52.78	52.32	50.50	47.93	45.08	42.20	20.57
	² B ₁	— ^b	71.46	76.89	82.17	87.13	90.49	91.38	90.94	89.90	88.55	81.16
mean ^c		9.75	7.72	7.68	8.52	9.88	10.83	10.82	10.32	9.67	9.02	10.26
mean— ² B ₁ ^d		9.75	8.21	7.14	6.38	5.96	5.45	4.58	3.54	2.57	2.02	9.26

^a See Table S1. ^b This state cannot be converged with the BLYP functional. ^c Standard deviation values have been calculated as $(\sum_{i=1}^N (E_i^{\text{level of theory}} - E_i^{\text{CCSD(T)}})^2/N)^{1/2}$ with $N = 6$ ($E(^2A'')$, $E(^2A')$, $E(^2A_2)$, $E(^2B_2)$, $E(^2A_1)$, $E(^2B_1)$). CCSD(T) relative energies used are those of Table 3. ^d The results of the ²B₁ state are not taken into account in the calculation of the STD.

charges of Table S8 in the Supporting Information. The ²A₁ and ²B₁ states remain essentially unmodified by variations of the a_0 parameter, except for the R_{O-O} bond distance in the ²B₁ state that increases for smaller a_0 values. The increase in the a_0 parameter leads to a stabilization of the 3d Cu and O₂ π orbitals. Since the stabilization is smaller for the 3d orbitals, one gets smaller amplitudes of the O₂ π orbitals (and higher for the intervening 3d orbitals) in the 4b₁ orbital which is singly occupied in the ²B₁ state. As a consequence, the R_{O-O} bond distance in this state is larger for smaller a_0 values.

In Table 8, we gather the STD of the geometrical parameters given in Table 6. The smaller STD values are attained for PS = 2–5 ($0.2 < a_0 < 0.5$), which is consistent with the fact that for the DFT methods tested previously the smaller STD values were obtained for B3LYP ($a_0 = 0.2$) and for B3LYP* ($a_0 = 0.15$).

The relative stability of the different electronic states found by different B3LYP-like functionals analyzed methods is the same as that found for the rest of DFT methods, i.e., $^2A''(C_s) < ^2A_2(C_{2v}) < ^2A'(C_s) < ^2B_2(C_{2v}) \ll ^2A_1(C_{2v}) < ^2B_1(C_{2v})$ (see Table 9). Although in all cases the ground state of CuO₂ is the ²A'', when we increase the a_0 parameter the difference in energy between the ²A'' and ²A₂ decreases. For the PS9, the values for the relative energies for the ²A'' and ²A₂ electronic states are quite close to the ones obtained with CCSD(T). We attributed this behavior to the larger ionic character of the ²A₂ state. Ionic states are overstabilized by the HF method. Therefore, a functional containing large proportion of HF exchange stabilizes the ²A₂ state as compared to the ²A'' state. Indeed, the HF method outperforms most of DFT functionals as far as the energy differences between ²A'' and ²A₂ is concerned. The increase in the a_0 parameter leads also to smaller energy differences between the ²A₂ and ²B₂ states. The reason can be found in the stabilization of the 3d Cu and O₂ π^* orbitals for

large a_0 values. The stabilization is slightly larger for the 3d orbitals, and this leads to larger amplitudes of the O₂ π^* orbitals (and smaller for the intervening 3d orbitals) in the 6b₂ and 2a₂ orbitals which are singly or doubly occupied in the ²A₂ and ²B₂ states. Thus, for larger a_0 values one has longer Cu–O bonds (*vide supra*) and more similar 6b₂ and 2a₂ orbitals, which become almost pure O₂ π^* orbitals. This leads to smaller energy differences between the ²A₂ and ²B₂ states (and the same for the ²A'' and ²A' states). The trends for the ²A₁ and ²B₁ states are less clear. In general, PS1, PS2, and PS3 ($0.1 < a_0 < 0.3$) are the parameter sets that globally give the most similar energies for the studied electronic states to the data obtained with the CCSD(T) method using the same 6-311+G(d) basis set. As it has been mentioned before, B3LYP ($a_0 = 0.2$) and B3LYP* ($a_0 = 0.15$) give, globally and among the DFT methods studied, the more similar results to the data obtained using CCSD(T). Somewhat unexpectedly, for relative energies the B3LYP-like functional with a larger contribution of exact exchange (90%) is the one giving the smaller standard deviation when the ²B₁ state is not included in the calculation. Binding energies obtained with the different PSs are collected in Table S19.

It is known that in odd-electron systems the self-interaction error (SIE) can be potentially important and artificially stabilize delocalized states. Hybrid functionals show smaller SIEs than pure functionals because they include a HF exchange portion. Therefore, one could hypothesize that the stabilization of the ²A₂ as compared to ²A'' when increasing the a_0 value (and also of the ²B₂ with respect to the ²A₂) is due to the effect of SIE. In Figure 3, the spin density on the Cu atom is depicted as a function of the a_0 parameter for the C_{2v} electronic states, respectively. As can be seen, we have three different situations. For the ²A₂ and ²B₂ electronic states (and the same occurs in the ²A'' and ²A' states), the increase of the a_0 parameter causes

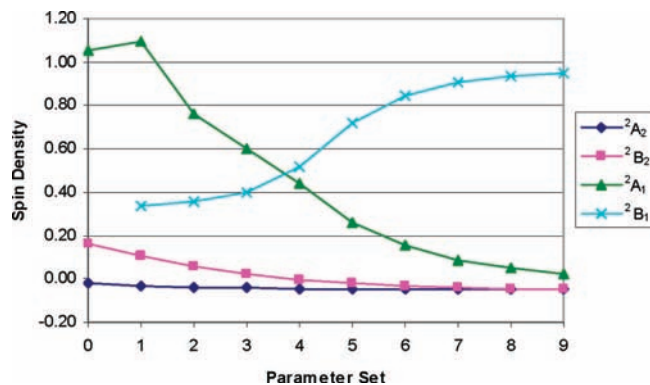


Figure 3. Spin density (au) at the Cu atom for the C_{2v} CuO₂ species in different electronic states computed with the B3LYP method using different parameter sets (see Table S2).

no change in the localization of the unpaired electron, since it remains completely localized on the O₂ moiety. So, this result indicates that the SIE should be similar for these states and should have no influence in the change of relative energies. On the other hand, for the 2A_1 electronic state, for low a_0 values the spin is on the copper, which means that basically we have Cu interacting with O₂. With the increase in the a_0 parameter, the 2A_1 electronic state evolves to Cu⁺ and O₂^{·-}. Finally, for the 2B_1 electronic state, the spin density on Cu⁺ increases from approximately 0.2 to 0.9 with the increase in the a_0 parameter, which is a consequence of the decrease of O participation in the 4b₁ for larger a_0 values.

In Table 10 we list the number of imaginary frequencies found for the located C_{2v} and C_s stationary points with the different methods used and for the set of electronic states analyzed. CCSD(T) frequencies have been computed by a numerical procedure. Since the asymmetric stretching mode breaks the C_{2v} symmetry, the numerical calculation of the frequencies is only possible for the two lowest-lying 2A_2 and 2B_2 states, which are related with the ${}^2A''$ and ${}^2A'$ states in C_s symmetry. It is interesting to verify that the nature of the functional and the percentage of HF exchange in B3LYP-like functionals modify the nature of the stationary points. Indeed, the HF, BLYP, G96LYP, OLYP, OPBE, mPWPW91, B3LYP, B3LYP*, M05, HCTH, TPSS, and B3LYP-like functionals with PS = 0–5 predict an imaginary frequency for the 2A_2 electronic state. So, this C_{2v} stationary point is found to be a transition state

connecting two ${}^2A''$ equivalent minima. Only the BHandH, VSXC, and B3LYP-like functionals with PS = 6–9 point out, like the CCSD(T) method, that this species is a minimum. On the other hand, HF and B3LYP-like functionals with PS = 4–9 indicate that the 2B_2 C_{2v} species is a transition state connecting two ${}^2A''$ equivalent minima. Indeed, only the BHandH and the VSXC functionals correctly predict the correct number (zero) of imaginary frequencies for the ${}^2A''$, ${}^2A'$, 2A_2 , and 2B_2 electronic states.

CONCLUSIONS

The ground and low-lying states of doublet CuO₂ have been studied using different density functional and CCSD(T) methods. At the CCSD(T) level, the CuO₂ doublet presents C_{2v} geometry and the ground electronic state is a 2A_2 state. The end-on C_s ${}^2A''$ electronic state lies, however, less than 1 kcal mol⁻¹ above. Moreover, at the CCSD(T) level of theory the relative order of the electronic states is ${}^2A_2(C_{2v}) < {}^2A''(C_s) < {}^2B_2(C_{2v}) < {}^2A'(C_s) \ll {}^2A_1(C_{2v}) < {}^2B_1(C_{2v})$. These results are reproduced by none of the DFT functionals that have been used, since in all cases the computed ground state is the ${}^2A''$ with an end-on C_s geometry. The reason for the DFT computed higher stability of the ${}^2A''$ relative to 2A_2 state cannot be attributed to a higher electron delocalization in the ${}^2A''$ state and must be ascribed to its larger covalent character. The relative energy between the $C_{2v}({}^2A_2)$ and $C_s({}^2A'')$ structures computed for the different functionals ranges between 2 and 16 kcal mol⁻¹, the functional that better compares with CCSD(T) being the BHandH one. However, when one compares the best geometries and relative energies with respect to CCSD(T) results for *all* the different electronic states analyzed, it is found that B3LYP gives the smallest standard deviations. As for the effect of the a_0 parameter, it is found that the B3LYP-like functional yielding better geometries contains 20% of exact exchange, although somewhat unexpectedly, and for relative energies the B3LYP-like functional with a larger contribution of exact exchange (90%) is the one giving the smaller standard deviation. Interestingly, only the BHandH and the VSXC functionals correctly predict the correct number (zero) of imaginary frequencies for the ${}^2A''$, ${}^2A'$, 2A_2 , and 2B_2 electronic states.

From our calculations it is clear that only high level *ab initio* methods providing a good estimation of correlation energy (such as MCSCF or CCSD) are able to give the correct relative energies of the different states in CuO₂. Since such methods

TABLE 10: Number of Imaginary Frequencies of the C_{2v} and C_s Stationary Points for the Ground State and Low-Lying Electronic States Considering the Different Methods Used

symmetry	state	HF	G96LYP	OLYP	OPBE	mPWPW91	B3LYP	B3LYP*	BHandH	M05	VSXC	HCTH	TPSS	CCSD(T)
C_s	${}^2A''$	0	0	0	0	0	0	0	0	0	0	0	0	0
	${}^2A'$	0	0	0	0	0	0	0	0	0	0	0	0	0
C_{2v}	2A_2	1	1	1	1	1	1	1	0	1	0	1	1	0
	2B_2	1	0	0	0	0	0	0	0	0	0	0	0	0
	2A_1	1	0	0	0	0	0	0	0	0	0	0	0	— ^a
	2B_1	0	0	0	0	0	0	0	0	0	0	0	0	— ^a
B3LYP														
symmetry	state	0	1	2	3	4	5	6	7	8	9			
C_s	${}^2A''$	0	0	0	0	0	0	0	0	0	0	0	0	0
	${}^2A'$	0	0	0	0	0	0	0	0	0	0	0	0	0
C_{2v}	2A_2	1	1	1	1	1	1	0	0	0	0	0	0	0
	2B_2	0	0	0	0	0	1	1	1	1	1	1	1	1
	2A_1	0	0	0	0	0	0	0	0	0	0	0	1	1
	2B_1	0	0	0	0	0	0	0	0	0	0	0	0	0

^a Calculations for these states are not possible because the numerical procedure breaks the symmetry of the molecule.

are usually not affordable for large $L_n\text{Cu}^I\text{-O}_2^{\cdot-}$ species, the functional of choice for these cases should be the B3LYP method for geometry optimizations followed by single-point calculations with a B3LYP-like functional containing a large percentage of HF exchange (for instance, PS 9).

Acknowledgment. This study was financially supported by the Spanish research projects CTQ2005-08797-C02-01/BQU and CTQ2008-03077/BQU and the DURSI project 2005SGR-00238. M.G. thanks the Spanish MEC for Ph.D. grant.

Supporting Information Available: Figure S1 with a schematic representation of interaction between the Cu (2S) and O_2 ($^3\Sigma_g^-$) fragments in the 2B_2 electronic state of the C_{2v} CuO_2 species. Tables S1–S19 with the parameter sets analyzed, the S^2 values, pictures of molecular orbitals for all electronic states, Mulliken charges, O–O bond distances in O_2 and O_2^- , calculated harmonic vibrational frequencies, ionization potentials, and binding energies for all electronic states analyzed. This material is available free of charge via the Internet at <http://pubs.acs.org>.

References and Notes

- Rosenzweig, A. C.; Sazinsky, M. H. *Curr. Opin. Struct. Biol.* **2006**, *16*, 729.
- MacPherson, I. S.; Murphy, M. E. P. *Cell. Mol. Life Sci.* **2007**, *64*, 2887.
- Punniyamurthy, T.; Velusamy, S.; Iqbal, J. *Chem. Rev.* **2005**, *105*, 2329.
- Holm, R. H.; Kennepohl, P.; Solomon, E. I. *Chem. Rev.* **1996**, *96*, 2239.
- Bento, I.; Carrondo, M. A.; Lindley, P. F. *J. Biol. Inorg. Chem.* **2006**, *11*, 539.
- Miller, A. F. *Curr. Opin. Chem. Biol.* **2004**, *8*, 162.
- Fridovich, I. *J. Biol. Chem.* **1997**, *272*, 18515.
- Hart, P. J.; Balbirnie, M. M.; Ogihara, N. L.; Nersissian, A. M.; Weiss, M. S.; Valentine, J. S.; Eisenberg, D. *Biochemistry* **1999**, *38*, 2167.
- Torrent, M.; Solà, M.; Frenking, G. *Chem. Rev.* **2000**, *100*, 439.
- Himo, F.; Siegbahn, P. E. M. *Chem. Rev.* **2003**, *103*, 2421.
- Siegbahn, P. E. M.; Blomberg, M. R. A. *Chem. Rev.* **2000**, *100*, 421.
- Siegbahn, P. E. M.; Blomberg, M. R. A. *Annu. Rev. Phys. Chem.* **1999**, *50*, 221.
- Poater, J.; Solà, M.; Rimola, A.; Rodríguez-Santiago, L.; Sodupe, M. J. *Phys. Chem. A* **2004**, *108*, 6072.
- Braida, B.; Hiberty, P. C.; Savin, A. *J. Phys. Chem. A* **1998**, *102*, 7872.
- Sodupe, M.; Bertran, J.; Rodríguez-Santiago, L.; Baerends, E. J. *J. Phys. Chem. A* **1999**, *103*, 166.
- Chermette, H.; Ciofini, I.; Mariotti, F.; Daul, C. *J. Chem. Phys.* **2001**, *115*, 11068.
- Bartlett, R. J. *Annu. Rev. Phys. Chem.* **1981**, *32*, 359.
- Raghavachari, K.; Trucks, G. W.; Pople, J. A.; Headgordon, M. *Chem. Phys. Lett.* **1989**, *157*, 479.
- Pouillon, Y.; Massobrio, C. *Chem. Phys. Lett.* **2000**, *331*, 290.
- Chertihin, G. V.; Andrews, L., Jr. *J. Phys. Chem. A* **1997**, *101*, 4026.
- Zhao, Y.; Truhlar, D. G. *Acc. Chem. Res.* **2008**, *41*, 157.
- Schultz, N. E.; Zhao, Y.; Truhlar, D. G. *J. Phys. Chem. A* **2005**, *109*, 11127.
- Schultz, N. E.; Zhao, Y.; Truhlar, D. G. *J. Phys. Chem. A* **2005**, *109*, 4388.
- Neese, F. *J. Biol. Inorg. Chem.* **2006**, *11*, 702.
- Quintal, M. M.; Karton, A.; Iron, M. A.; Boese, A. D.; Martin, J. M. L. *J. Phys. Chem. A* **2006**, *110*, 709.
- Zhao, Y.; Truhlar, D. G. *J. Chem. Phys.* **2006**, *124*, 224105.
- Zhao, Y.; Truhlar, D. G. *Theor. Chem. Acc.* **2008**, *120*, 215.
- Tevault, D. E. *J. Chem. Phys.* **1982**, *76*, 2859.
- Howard, J. A.; Sutcliffe, R.; Mile, B. *J. Phys. Chem.* **1984**, *88*, 4351.
- Kasai, P. H.; Jones, P. M. *J. Phys. Chem.* **1986**, *90*, 4239.
- Mattar, S. M.; Ozin, G. A. *J. Phys. Chem.* **1988**, *92*, 3511.
- Ozin, G. A.; Mitchell, S. A.; Garcia-Prieto, J. *J. Am. Chem. Soc.* **1983**, *105*, 6399.
- Wu, H.; Desai, S. R.; Wang, L.-S. *J. Phys. Chem. A* **1997**, *101*, 2103.
- Bondybey, V. E.; English, J. H. *J. Phys. Chem.* **1984**, *88*, 2247.
- Uzunova, E. L.; Mikosch, H.; Nikolov, G. S. *J. Chem. Phys.* **2008**, *128*, 094307.
- Mitchell, S. A. *Gas Phase Metal Reactions*; Fontijn, A., Ed.; Elsevier: Amsterdam, 1992.
- Hamsegawa, J.; Pierloot, K.; Roos, B. O. *Chem. Phys. Lett.* **2001**, *335*, 503.
- Barone, V.; Adamo, C. *J. Phys. Chem.* **1996**, *100*, 2094.
- Mochizuki, Y.; Nagashima, U.; Yamamoto, S.; Kashiwagi, H. *Chem. Phys. Lett.* **1989**, *164*, 225.
- Bauschlicher, C. W., Jr.; Langhoff, S. R.; Partridge, H.; Sodupe, M. J. *Phys. Chem.* **1993**, *97*, 856.
- Hrusák, J.; Koch, W.; Schwarz, H. *J. Chem. Phys.* **1994**, *101*, 3898.
- Poater, J.; Solà, M.; Duran, M.; Robles, J. *Phys. Chem. Chem. Phys.* **2002**, *4*, 722.
- Latajka, Z.; Bouteiller, Y.; Scheiner, S. *Chem. Phys. Lett.* **1995**, *234*, 159.
- Lundell, J.; Latajka, Z. *J. Phys. Chem. A* **1997**, *101*, 5004.
- Hoe, W. M.; Cohen, A. J.; Handy, N. C. *Chem. Phys. Lett.* **2001**, *341*, 319.
- Csonka, G. I.; Nguyen, N. A.; Kolossváry, I. *J. Comput. Chem.* **1997**, *18*, 1534.
- Chermette, H.; Razafinjanahary, H.; Carrion, L. *J. Chem. Phys.* **1997**, *107*, 10643.
- Poater, J.; Duran, M.; Solà, M. *J. Comput. Chem.* **2001**, *22*, 1666.
- Durant, J. L. *Chem. Phys. Lett.* **1996**, *256*, 595.
- Lynch, B. J.; Truhlar, D. G. *J. Phys. Chem. A* **2001**, *105*, 2936.
- Lynch, B. J.; Fast, P. L.; Harris, M.; Truhlar, D. G. *J. Phys. Chem. A* **2000**, *104*, 4811.
- Kormos, B. L.; Cramer, C. J. *J. Phys. Org. Chem.* **2002**, *15*, 712.
- Kalaiselvan, A.; Venuvanalingam, P.; Poater, J.; Solà, M. *Int. J. Quantum Chem.* **2005**, *102*, 139.
- Abu-Awwad, F.; Politzer, P. *J. Comput. Chem.* **2000**, *21*, 227.
- Dkhissi, A.; Alikhani, M. E.; Bouteiller, Y. *J. Mol. Struct. (Theochem)* **1997**, *416*, 1.
- Wilson, P. J.; Tozer, D. J. *J. Chem. Phys.* **2002**, *116*, 10139.
- Reiher, M.; Salomon, O.; Hess, B. A. *Theor. Chem. Acc.* **2001**, *107*, 48.
- Becke, A. D. *J. Chem. Phys.* **1993**, *98*, 5648.
- Reiher, M. *Inorg. Chem.* **2002**, *41*, 6928.
- Swart, M.; Groenhof, A. R.; Ehlers, A. W.; Lammertsma, K. J. *Phys. Chem. A* **2004**, *108*, 5479.
- Handy, N. C.; Cohen, A. J. *Mol. Phys.* **2001**, *102*, 403.
- Perdew, J. P.; Burke, K.; Ernzerhof, M. *Phys. Rev. Lett.* **1996**, *77*, 3865.
- Güell, M.; Luis, J. M.; Solà, M.; Swart, M. J. *Phys. Chem. A* **2008**, *112*, 6384.
- Frisch, M. J.; Trucks, G. W.; Schlegel, H. B.; Scuseria, G. E.; Robb, M. A.; Cheeseman, J. R.; Montgomery, J. A., Jr.; Vreven, T.; Kudin, K. N.; Burant, J. C.; Millam, J. M.; Iyengar, S. S.; Tomasi, J.; Barone, V.; Mennucci, B.; Cossi, M.; Scalmani, G.; Rega, N.; Petersson, G. A.; Nakatsuji, H.; Hada, M.; Ehara, M.; Toyota, K.; Fukuda, R.; Hasegawa, J.; Ishida, M.; Nakajima, T.; Honda, Y.; Kitao, O.; Nakai, H.; Klene, M.; Li, X.; Knox, J. E.; Hratchian, H. P.; Cross, J. B.; Bakken, V.; Adamo, C.; Jaramillo, J.; Gomperts, R.; Stratmann, R. E.; Yazyev, O.; Austin, A. J.; Cammi, R.; Pomelli, C.; Ochterski, J. W.; Ayala, P. Y.; Morokuma, K.; Voth, G. A.; Salvador, P.; Dannenberg, J. J.; Zakrzewski, G.; Dapprich, S.; Daniels, A. D.; Strain, M. C.; Farkas, O.; Malick, D. K.; Rabuck, A. D.; Raghavachari, K.; Foresman, J. B.; Ortiz, J. V.; Cui, Q.; Baboul, A. G.; Clifford, S.; Cioslowski, J.; Stefanov, B. B.; Liu, G.; Liashenko, A.; Piskorz, P.; Komaromi, I.; Martin, R. L.; Fox, D. J.; Keith, T.; Al-Laham, M. A.; Peng, C. Y.; Nanayakkara, A.; Challacombe, M.; Gill, P. M. W.; Johnson, B.; Chen, W.; Wong, M. W.; Gonzalez, C.; Pople, J. A. *Gaussian 03*, revision C.01; Gaussian, Inc.: Pittsburgh, PA, 2003.
- Werner, H.-J.; Knowles, P. J.; Lindh, R.; Manby, F. R.; Schütz, M. *MOLPRO*, version 2006.1, a package of ab initio programs, 2006.
- Wachters, A. J. H. *J. Chem. Phys.* **1970**, *52*, 1033.
- In the Gaussian 03 implementation of the Cu basis set, the s and p functions come from Wachter's optimization for the Cu atom in its 2S state, while the d functions come from Wachter's optimization for the Cu atom in its 2D state. In addition, we have checked that with the B3LYP method the Gaussian 03 internal basis set provides more reasonable results for the relative energies among the different analyzed states than the basis set with the d functions coming from Wachter's optimization for the Cu atom in its 2D state.
- Dunning, T. H., Jr. *J. Chem. Phys.* **1989**, *90*, 1007.
- Halkier, A.; Helgaker, T.; Jørgensen, P.; Klopper, W.; Koch, H.; Olsen, J.; Wilson, A. K. *Chem. Phys. Lett.* **1998**, *286*, 243.
- Lee, C. T.; Yang, W. T.; Parr, R. G. *Phys. Rev. B* **1988**, *37*, 785.
- Becke, A. D. *Phys. Rev. A* **1988**, *38*, 3098.
- Perdew, J. P.; Chevary, J. A.; Vosko, S. H.; Jackson, K. A.; Pederson, M. R.; Singh, D. J.; Fiolhais, C. *Phys. Rev. B* **1992**, *46*, 6671.

- (73) Perdew, J. P.; Chevary, J. A.; Vosko, S. H.; Jackson, K. A.; Pederson, M. R.; Singh, D. J.; Fiolhais, C. *Phys. Rev. B* **1993**, *48*, 4978.
- (74) Perdew, J. P.; Burke, K.; Wang, Y. *Phys. Rev. B* **1998**, *57*, 14999.
- (75) Perdew, J. P.; Burke, K.; Wang, Y. *Phys. Rev. B* **1996**, *54*, 16533.
- (76) Stephens, P. J.; Devlin, F. J.; Chabalowski, C. F.; Frisch, M. J. *J. Phys. Chem.* **1994**, *98*, 11623.
- (77) Vosko, S. H.; Wilk, L.; Nusair, M. *Can. J. Phys.* **1980**, *58*, 1200.
- (78) Hertwig, R. H.; Koch, W. *Chem. Phys. Lett.* **1997**, *268*, 345.
- (79) Burke, K.; Ernzerhof, M.; Perdew, J. P. *Chem. Phys. Lett.* **1997**, *265*, 115.
- (80) Gill, P. M. W. *Mol. Phys.* **1996**, *89*, 433.
- (81) Perdew, J. P.; Wang, Y. *Phys. Rev. B* **1992**, *45*, 13244.
- (82) Becke, A. D. *J. Chem. Phys.* **1993**, *98*, 1372.
- (83) Zhao, Y.; Schultz, N. E.; Truhlar, D. G. *J. Chem. Phys.* **2005**, *126*, 161103.
- (84) Van Voorhis, T.; Scuseria, G. E. *J. Chem. Phys.* **1998**, *109*, 400.
- (85) Hamprecht, F. A.; Cohen, A. J.; Tozer, D. J.; Handy, N. C. *J. Chem. Phys.* **1998**, *109*, 6264.
- (86) Tao, J. M.; Perdew, J. P.; Staroverov, V. N.; Scuseria, G. E. *Phys. Rev. Lett.* **2003**, *91*, 146401.
- (87) Zhao, Y.; Schultz, N. E.; Truhlar, D. G. *J. Chem. Theory Comput.* **2006**, *2*, 364.
- (88) Lee, T. J.; Rice, J. E.; Scuseria, G. E.; Schaefer, H. F., III. *Theor. Chim. Acta* **1989**, *75*, 81.
- (89) Huber, K. P.; Herzberg, G. *Molecular spectra and molecular structure*; Van Nostrand Reinhold: New York, 1979; Vol. 4.
- (90) *CRC Handbook of Chemistry and Physics*, 79th ed.; Lide, D. R., Ed.; CRC Press: Boca Raton, FL, 1998.
- (91) Ervin, K. M.; Anusiewicz, I.; Skurski, P.; Simons, J.; Lineberger, W. C. *J. Phys. Chem. A* **2003**, *107*, 8521.
- (92) Salzner, U.; Lagowski, J. B.; Pickup, P. G.; Poirier, R. A. *J. Comput. Chem.* **1997**, *18*, 1943.
- (93) Becke, A. D. *J. Chem. Phys.* **1996**, *104*, 1040.

JP8031379